

An elongated tract of polyQ in the carboxyl-terminus of human α 1A calcium channel induces cell apoptosis by nuclear translocation

Ji Sun¹, Xiguang Sun², Zhuo Li³, Dihui Ma^{4*} and Yudan Lv^{4*}

Departments of ¹Pediatric Neurology, ²Hand Surgery, ³Endocrinology and Metabolism, and ⁴Neurology, The First Hospital of Jilin University, Changchun, Jilin 130021, P.R. China

Received September 6, 2019; Accepted March 5, 2020

DOI: 10.3892/or.2020.7592

Abstract. An aberrant elongated tract of glutamine residues (polyQ) in proteins induces multiple diseases treated in the clinic. In our previous study of progressive myoclonic epilepsy (PME), using whole-exome sequencing, a mutant Cav2.1 protein with an aberrant elongated polyQ tract was identified in PME patients. To investigate the molecular mechanism and cell biology of this aberrant elongated polyQ tract, wild-type Cav2.1 with 13 polyQ repeats (Cav2.1 wt-Q13) and mutant-type Cav2.1 with 26 polyQ repeats (Cav2.1 mt-Q26) were prepared and introduced into human SH-SY5Y neuroblastoma cells. Using a WST-1 assay, it was revealed that Cav2.1 mt-Q26 markedly suppressed the proliferation of the SH-SY5Y cells, a result not observed for the Cav2.1 wt-Q13-transfected cells. It was also revealed that Cav2.1 mt and its truncated molecules suppressed cell proliferation by inducing apoptosis rather than arresting the cell cycle. Further investigations indicated a nuclear translocation phenomenon associated with the Cav2.1 mt molecules. Mechanistically, it was revealed that the Cav2.1 mt molecules activated the Bcl-2/Bax, caspase-3 and poly ADP-ribose polymerase (PARP) apoptotic pathways. The present study may provide new insights for interpreting the pathogenesis of PME and the relationship among polyQ, *CACNA1A* gene mutations and PME.

Introduction

The *CACNA1A* gene, located on chromosome 19p13, encodes the pore-forming α -1A subunit of human neuronal voltage-gated

Cav2.1 (P/Q-type) calcium channels (1,2). Mutations in the *CACNA1A* gene cause several autosomal-dominant neurological disorders and clinical symptoms/phenotypes such as migraines, spinocerebellar ataxia, familial hemiplegic migraine (FHM), and episodic ataxia (EA) (3-6).

In our previous study, using whole-exome sequencing, a homozygous variant of Cav2.1 was identified in a three-generation consanguineous Chinese Han family with progressive myoclonic epilepsy (PME), which is a heterogeneous neurodegenerative disorder (7). The mutant Cav2.1 was revealed in two siblings but not in fifty normal donors, indicating the mutation gene spectrum of *CACNA1A* can be used as a valuable predictor for PME.

A repeated polymorphic cytosine-adenine-guanine (CAG) mutation was also identified in the PME patient samples that encodes an elongated tract of glutamine residues in the C-terminus of Cav2.1. It has been suggested that trinucleotide repeat expansion in the CAG in protein coding regions in the genome may cause polyglutamine (polyQ) disease, which induces a set of dominantly inherited neurodegenerative disorders including Huntington's disease (HD), spinocerebellar ataxia, type 1/2/3/6/7 (SCA-1/2/3/6/7), dentatorubropallidoluysian atrophy (DRPLA), Machado-Joseph disease (MJD) and spinobulbar muscular atrophy (8,9).

Although polyQ diseases are well known clinically, their molecular mechanism and cell biological behavior are still unclear, especially in the context of PME. To address this issue, in the present study, a wild-type (wt) human Cav2.1 (Cav2.1 wt) with 13 repeats of CAG as well as a mutant-type (mt) Cav2.1 (Cav2.1 mt) with 26 repeats of CAG in the C-terminus of this protein were constructed and delivered into cells of the SH-SY5Y neuroblastoma cell line, which is always used as the model cell line for investigations of human nervous system diseases (10-12). The results revealed that the forced expression of Cav2.1 mt significantly inhibited SH-SY5Y cell proliferation by inducing apoptosis. By constructing a series of truncated Cav2.1 mt molecules and a Cav2.1 mt-GFP fusion molecule, a marked nuclear translocation phenomenon was revealed. Furthermore, it was observed that Cav2.1 mt may activate apoptosis-relevant factors, namely, Bcl-2/Bax, caspase and PARP, and thus induces cell apoptosis. The present study clearly revealed the apoptosis-inducing effects of polyQ

Correspondence to: Professor Dihui Ma or Professor Yudan Lv, Department of Neurology, The First Hospital of Jilin University, 1 Xinmin Street, Changchun, Jilin 130021, P.R. China
E-mail: madihui@126.com
E-mail: lvyudan@sina.com

*Contributed equally

Key words: *CACNA1A*, polyglutamine, cell apoptosis, nuclear translocation

mutations in human nerve cells, a finding that may provide a new insight useful for interpreting the pathogenesis of and developing new therapeutic targets for PME.

Materials and methods

Cell culture. Human SH-SY5Y neuroblastoma cells were kindly provided by the Stem Cell Bank, Chinese Academy of Sciences (cat. no. SCSP-5014) and were authenticated by STR profiling (Shanghai Genechem Co., Ltd.). The cells were routinely maintained in Dulbecco's modified Eagle's medium (DMEM; GE Healthcare Life Sciences) supplemented with 10% fetal calf serum (FCS; GE Healthcare Life Sciences), 100 μ g/ml streptomycin and 100 U/ml penicillin (HyClone; GE Healthcare Life Sciences) under standard conditions (37°C, 5% CO₂). The cell culture medium was changed every two days. Upon reaching 80% confluence, the cells were digested with 0.25% trypsin (GE Healthcare Life Sciences) for 1 min at 37°C.

Plasmid construction. The DNA molecules expressing Cav2.1 wt (Q13, 13 CAG repeats) and Cav2.1 mt (Q26, 26 CAG repeats) were synthesized by Sangon Biotech Co., Ltd. The first CAG starts from the 6955 site of *CACNA1A* cDNA (NM_023035.2). DNA molecules were cloned into pcDNA3.1.neo vector with *Bam*HI and *Xba*I restriction enzyme sites. The DNA expressing a series of *CACNA1A* deletion mutants (Cav2.1dm) were synthesized by PCR reaction and cloned into pcDNA3.1.neo vector with *Bam*HI and *Xba*I. The primer sequences of the Cav2.1dm were as follows: Cav2.1N forward, 5'-CAAGGGATCCGCCACCATGGCCCGCTTCGGAGAC-3' and reverse, 5'-GCCCCTCTAGATTAGGCCTTACGGATCACAGG-3'; Cav2.1dm1 forward, 5'-CAAGGGATCCGCCACCATGCAGGTGTTTGGTAACATTG-3' and reverse, 5'-GCCCCTCTAGATTAGCACCAATCATCGTCAC-3'; Cav2.1dm2 forward, 5'-CAAGGGATCCGCCACCATGAAGCGTTCAGCCTCCG-3' and reverse, 5'-GCCCTCTAGATTAGCACCAATCATCGTCAC-3'; Cav2.1C forward, 5'-CAAGGGATCCGCCACCATGGCGGTGGCAGGCCGGGC-3' and reverse, 5'-GCCCCTCTAGATTAGCACCAATCATCGTCAC-3'. DNA sequences of Cav2.1dm3, Cav2.1dm4 and Cav2.1dm5 were synthesized by Sangon Biotech Co., Ltd. and cloned into the same vector via *Bam*HI and *Xba*I restriction enzyme sites. To ascertain the cellular distribution of Cav2.1dm, GFP was fused to the C-terminus of the Cav2.1dm3 molecule. The plasmid expressing Cav2.1dm3G fusion protein was constructed.

Polypeptide structure prediction. The 3D structure of polypeptide was built using an online tool (<http://zhanglab.cmb.med.umich.edu/>).

Transfection. According to the manufacturer's instructions, 2 μ g of each of the aforementioned plasmids and the empty vector (EV, control) were transfected into SH-SY5Y cells using Lipofectamine 3000 (Invitrogen; Thermo Fisher Scientific, Inc.). All the cellular experiments were carried out at or after 48 h post-transfection.

RNA extraction, reverse transcriptional reaction and real-time quantitative PCR (qPCR). Total RNA was isolated using

EasyPureRNA Purification Kit (cat. no. ER701; Beijing TransGen Biotech Co., Ltd.). RNA (1,000 ng) was reverse-transcribed with TransScript All-in-One First-Strand cDNA Synthesis SuperMix for qPCR (One-Step gDNA Removal) (cat. no. AT341; Beijing TransGen Biotech Co., Ltd.). qPCR was conducted based on the instructions of RealStar Green Fast Mixture (GenStar). Primers for qPCR are listed as follows: Forward primer for Cav2.1 wt, Cav2.1 mt, Cav2.1N, and Cav2.1dm4 is 5'-AAGGATCGGAAGCATCGACAG-3' and reverse primer is 5'-GTGCTGGTACCA GATGTTGAG-3'; forward primer for Cav2.1dm1, Cav2.1dm2, Cav2.1dm3, Cav2.1C and Cav2.1dm5 is 5'-GACTCCCCA ACGGCTACTAC-3' and reverse primer is 5'-CACCAATCA TCGTCACTCTCG-3'. qPCR was performed on ABI 7500 (Applied Biosystems; Thermo Fisher Scientific, Inc.) and the PCR program consisted of 10 sec at 95°C, 40 cycles at 95°C for 5 sec and 60°C for 35 sec. The relative expression of the aforementioned target gene was calculated based on the 2^{- $\Delta\Delta C_q$} method (13).

Cell growth assay. At 48 h post-transfection, SH-SY5Y cells were trypsinized and seeded into a 96-well plate at a density of 5x10³ cells/well and cultured for another 48 h. Cell proliferation was determined using WST-1 cell proliferation reagent (Roche Applied Science). According to the manufacturer's instructions, 20 μ l WST-1 was added to 200 μ l cell culture medium and incubated at 37°C in the dark for 2.5 h. The absorbances at 450 and 630 nm were assessed by a microplate reader (BioTek Instruments). The final OD (optical density) was designated as OD₄₅₀-OD₆₃₀-OD_{blank}.

Cell cycle and apoptosis assay. At 72 h post-transfection, at least 2x10⁶ cells were harvested and washed with phosphate-buffered saline (PBS) three times. For cell cycle analysis, cell pellets were resuspended in 200 μ l PBS containing 10 μ g/ml propidium iodide (PI; Sigma-Aldrich; Merck KGaA) and incubated for 30 min in the dark at room temperature. For cell apoptosis, the transfected cells were stained with an Annexin V-FITC/PI Apoptosis Detection kit (BD Biosciences) for 15 min in the dark and analyzed using a flow cytometer (FACScan; BD Biosciences) with FlowJo analysis software (version 10.0; FlowJo LLC). The cells in the quadrants represented the different cell states as follows: Late-apoptotic cells were presented in the upper right quadrant, viable cells were presented in the lower left quadrant, and early apoptotic cells were presented in the lower right quadrant.

Protein extraction. Protein was extracted from the whole cell, cell membrane, or cell nucleus of the SH-SY5Y cells, respectively. The whole cell protein was extracted with a Protein Extraction kit (cat. no. KGP2100; Nanjing KeyGen Biotech. Co., Ltd.). Cell membrane protein and nucleoprotein were extracted with a Cell Membrane Protein/Cytoplasmic Protein/Nucleoprotein Extraction kit (cat. no. KGBSP002; Nanjing KeyGen Biotech. Co., Ltd.).

Western blotting. Equal amounts of 25 μ g protein from each sample were loaded to 10% SDS polyacrylamide gel and separated by electrophoresis. Then, proteins were transferred to PVDF membranes (EMD Millipore). The membranes were incubated in 5% BSA (cat. no. E661003; Sangon

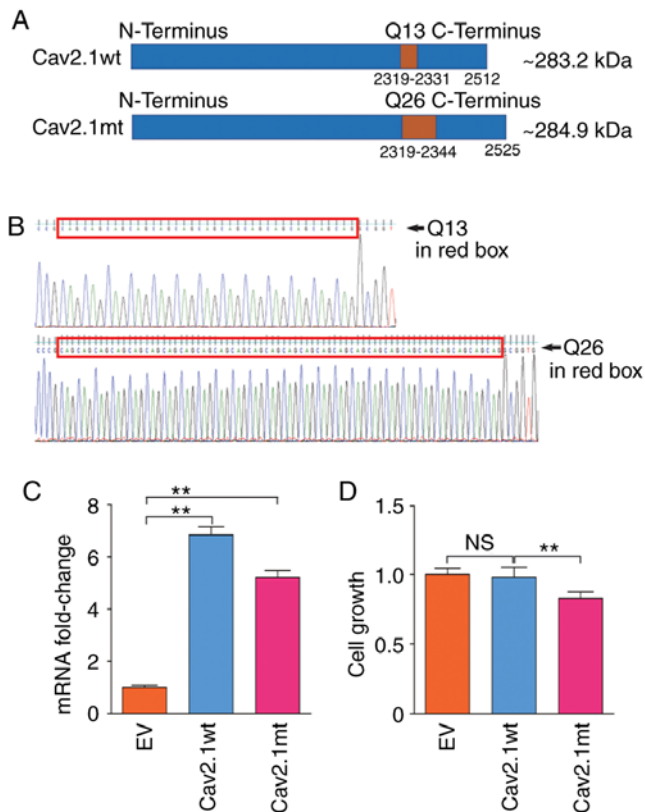


Figure 1. The forced expression of Cav2.1 mt-Q26 suppresses the proliferation of the SH-SY5Y cells compared with the Cav2.1 wt-Q13 and the EV transfectants. (A) Diagram of the structures of Cav2.1 wt and Cav2.1 mt molecules. (B) Sanger sequencing result of the Cav2.1 wt and Cav2.1 mt-expressing plasmid. The sequences in the red boxes indicate that the 13 and 26 CAG repeats were successfully synthesized and inserted into the pcDNA3.1 vector. (C) mRNA expression levels of Cav2.1 wt and Cav2.1 mt in the transfectant cells were confirmed by qPCR (t-test). (D) WST-1 assay indicated that the forced expression of Cav2.1 mt-Q26 suppressed SH-SY5Y cell proliferation (LSD test). ** $P < 0.01$. Cav2.1 mt-Q26, mutant-type Cav2.1 with 26 polyQ repeats; Cav2.1 wt-Q13, wild-type Cav2.1 with 26 polyQ repeats; CAG, cytosine-adenine-guanine; EV, empty vector; NS, no significance.

Biotech Co., Ltd.)/TBST solution at 37°C for 1 h and then washed in TBST 3 times for 5 min. The membranes were then incubated with primary antibodies at 4°C overnight. The primary antibodies were: Anti-Cav2.1 N-terminus (product code ab191140; recognizes Human CACNA1A aa 430-447; 1:1,500); anti-Cav2.1 C-terminus (product code ab181371; recognizes Human CACNA1A aa 2050-2150; 1:1,000); anti-Bcl-2 rabbit polyclonal antibody (product code ab59348; 1:15,000); and anti-Bax (product code ab32503; 1:1,500; all from Abcam); anti-cleaved caspase-3 (product no. 9664; 1:1,000; Cell Signaling Technology, Inc.); anti-cleaved poly ADP-ribose polymerase (PARP) (product code ab32064; 1:1,500); anti-GFP (product code ab6556, 1:3,000); and anti-β-actin (product code ab8226, 1:3,000; all from Abcam). After washing in TBST 3 times for 5 min, the membranes were incubated with HRP-coupled goat anti-rabbit or goat anti-mouse secondary antibody (cat. no. A0208 and cat. no. A0216, respectively; 1:2,000; Beyotime Institute of Biotechnology) at room temperature for 45 min. The chemiluminescence signals of the target proteins were visualized using ChemiDoc XRS+ system (Bio-Rad Laboratories, Inc.). Densitometric values of the blots were analyzed using

Quantity One software (version 4.6; Bio-Rad Laboratories, Inc.).

Immunofluorescence staining and nuclear counterstain. Cav2.1dm3G transfectants (5×10^5) in a six-well plate were washed with 2 ml cold PBS 2 times for 2 min and fixed with 3.7% formaldehyde for 15 min at room temperature (RT) (Sigma-Aldrich; Merck KGaA) in PBS. After the fixation buffer was removed, the cells were washed with PBS another 2 times for 2 min. Then, the cells were incubated with 0.5% Triton X-100 (Sigma; Merck KGaA) in PBS for 10 min at room temperature and washed with PBS 3 times for 2 min. Cells were blocked with 5% powdered milk in TBST buffer (Sangon Biotech Co., Ltd.) plus 0.02% sodium azide (Sigma-Aldrich; Merck KGaA) for 45 min at RT. After the blocking buffer was removed, the cells were incubated with TBST buffer containing anti-Cav2.1 antibody (1:800; cat. no. HPA064258; Sigma-Aldrich; Merck KGaA) for 1 h at RT. After washing 3 times for 5 min, the cells were incubated with TBST/0.5% BSA diluted Alexa Fluor 555 conjugate goat anti-rabbit IgG secondary antibody (cat. no. A-21428; Thermo Fisher Scientific, Inc.) at a concentration of 4 μg/ml (according to the manufacturer's instructions) for 45 min at RT.

To visualize the intracellular location of Cav2.1dm3G, cell nuclei were stained with DAPI. According to the manufacturer's instructions, SH-SY5Y cells expressing Cav2.1dm3G were washed with PBS 2 times for 2 min and 1.5 ml DAPI (Beyotime Institute of Biotechnology) was added to the wells. Then the cells were maintained at room temperature for 5 min.

An Olympus IX83 fluorescence microscope (Olympus Corporation) was used to observe the cellular morphology and fluorescence.

Statistical analysis. Statistical analysis was conducted with SPSS 17.0 software (SPSS, Inc.). All data were expressed as the mean ± standard deviation. All of the experiments were performed in triplicate and repeated at least three times. Significance was determined using Student's t-test or one-way analysis of variance (ANOVA) followed by LSD or Tukey's post hoc test. $P < 0.05$ and $P < 0.01$ were considered to indicate statistically significant differences (* $P < 0.05$ and ** $P < 0.01$ as indicated in the images and figure legends).

Results

Cav2.1 mt with 26 polyQ repeats suppresses the proliferation of the SH-SY5Y cells. The DNA molecules expressing Cav2.1 wt and Cav2.1 mt were synthesized and confirmed by Sanger sequencing (Fig. 1A and B). After the two expressing plasmids, pcDNA3.1-Cav2.1 wt and pcDNA3.1-Cav2.1 mt, were delivered into SH-SY5Y cells and confirmed by qPCR (Fig. 1C) cell proliferation was analyzed. As revealed in Fig. 1D, compared with the Cav2.1 wt-Q13 and the EV transfectants, the forced expression of Cav2.1 mt-Q26 significantly decreased the cell proliferation of the SH-SY5Y cells ($P < 0.01$).

Biological function of the truncated Cav2.1 mt molecules. It has been reported that Cav2.1 truncating mutation is associated with neurological disorders (14). Herein, to address whether the truncated Cav2.1 mt molecules affect the biological functions

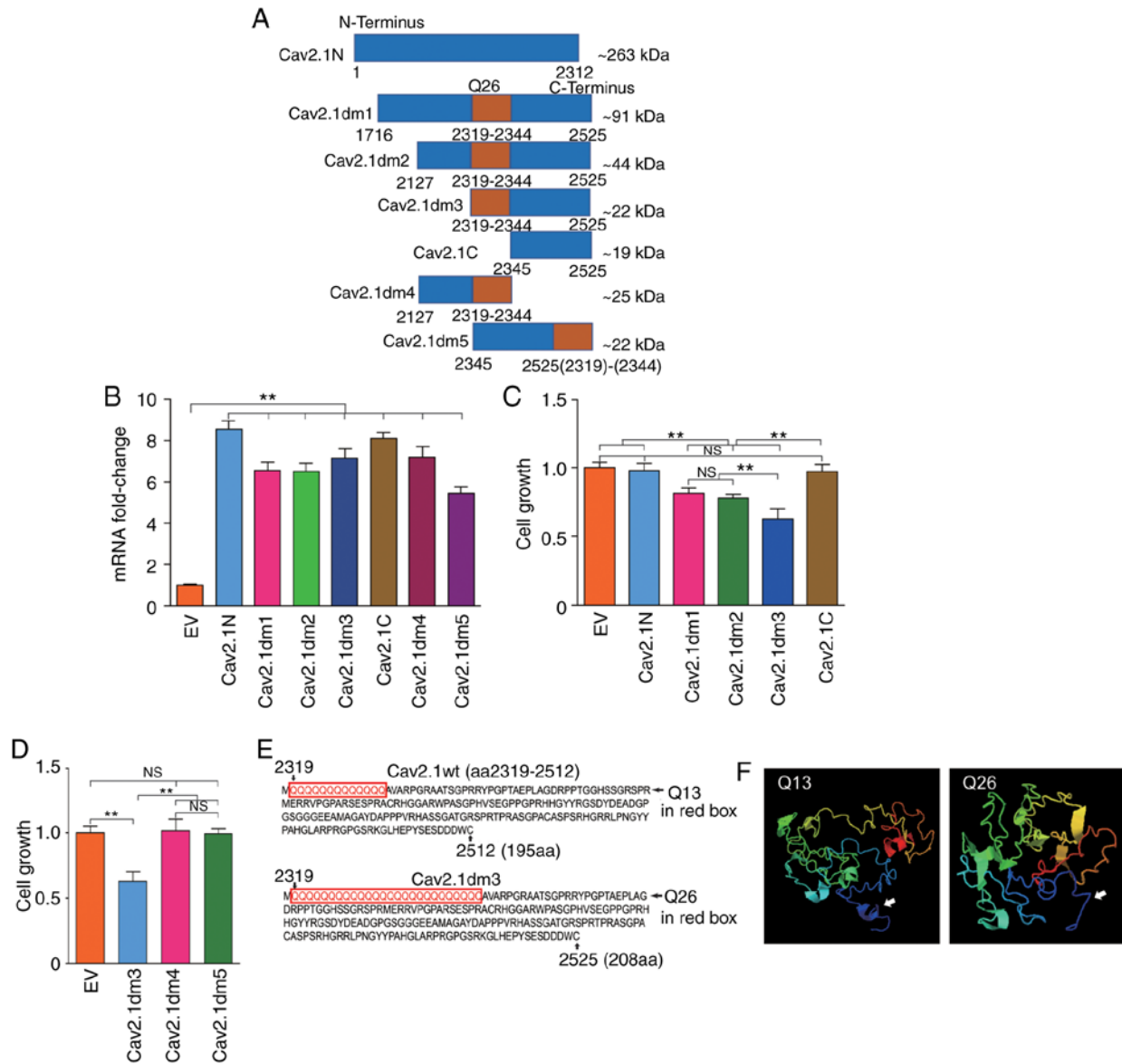


Figure 2. Construction of a series of truncated Cav2.1 mt molecules and addressing their effects on cell proliferation. (A) Diagram of the structures of seven truncated Cav2.1 mt molecules, an ~263 kDa N-terminus of Cav2.1 without polyQ repeat (Cav2.1N), a ~91 kDa C-terminus of Cav2.1 mt with 26 polyQ repeats (Cav2.1dm1), an ~44 kDa C-terminus of Cav2.1 mt with 26 polyQ repeats (Cav2.1dm2), an ~22 kDa C-terminus of Cav2.1 mt beginning with Q26 (Cav2.1dm3), an ~19 kDa C-terminus of Cav2.1 mt without polyQ repeat (Cav2.1C), an ~25 kDa C-terminus of Cav2.1 mt ending with Q26 (Cav2.1dm4) and a reversely assembled Cav2.1dm3 ending with Q26 (Cav2.1dm5). (B) mRNA expression levels of Cav2.1N, Cav2.1dm1, Cav2.1dm2, Cav2.1dm3, Cav2.1C, Cav2.1dm4 and Cav2.1dm5 in the transfected cells were confirmed by qPCR (t-test). (C) Comparison of proliferation of the SH-SY5Y cells transfected with a series of truncated Cav2.1 mt molecules. The WST-1 result indicated that Cav2.1N and Cav2.1C, containing no polyQ repeat did not affect the cell proliferation of the SH-SY5Y cells. Conversely, the forced expression of Cav2.1dm1, Cav2.1dm2 and Cav2.1dm3, containing 26 polyQ repeats significantly impaired cell proliferation. ** $P < 0.01$, a significant difference in cell proliferation was observed between EV/Cav2.1N/Cav2.1C and Cav2.1dm1/Cav2.1dm2/Cav2.1dm3, and Cav2.1dm1/Cav2.1dm2 and Cav2.1dm3. NS, no difference of cell proliferation was observed among EV, Cav2.1N and Cav2.1C, and Cav2.1dm1 and Cav2.1dm2 (Tukey's test). (D) Comparison of the proliferation of the SH-SY5Y cells transfected with Cav2.1dm3 and its two variations. The result indicated that only those molecules composed with integrity Q26 and C-terminus of Cav2.1 harbored cytotoxicity (Tukey's test). (E) Partial amino acid sequences of Cav2.1 wt-Q13 and Cav2.1dm3-Q26. (F) Comparison of the 3D structure of Cav2.1 wt and Cav2.1dm3. White arrows indicate the differences on the secondary structure between Q13 and Q26. ** $P < 0.01$. Cav2.1mt, mutant-type Cav2.1; Cav2.1 wt, wild-type Cav2.1; EV, empty vector; NS, no significance.

of the SH-SY5Y cells, a series of *CACNA1A* gene deletion mutations were prepared and the corresponding expressing plasmids that are schematically represented in Fig. 2A, were constructed. Cav2.1N is the aa1 to aa2312 on the N-terminus of Cav2.1 containing no polyQ; Cav2.1dm1 is the aa1716 to aa2525 of Cav2.1 mt containing 26 polyQ repeats; Cav2.1dm2 is the aa2127 to aa2525 of Cav2.1 mt containing 26 polyQ repeats; Cav2.1dm3 is the aa2319 to aa2525 of Cav2.1 mt, starting from the first Q and containing 26 polyQ repeats;

Cav2.1C is the aa2345 to aa2525 on the C-terminus of Cav2.1 containing no polyQ. The approximate molecular weight (kDa) of each deletion mutation was calculated by an online tool (http://www.detaibio.com/sms2/protein_mw.html). SH-SY5Y cells were then transfected with all the aforementioned plasmids and the transfection efficacy was confirmed by qPCR (Fig. 2B). The cell proliferation of all the transfected cells were detected by WST-1 and the result indicated that Cav2.1N and Cav2.1C, containing no polyQ repeats, did not affect

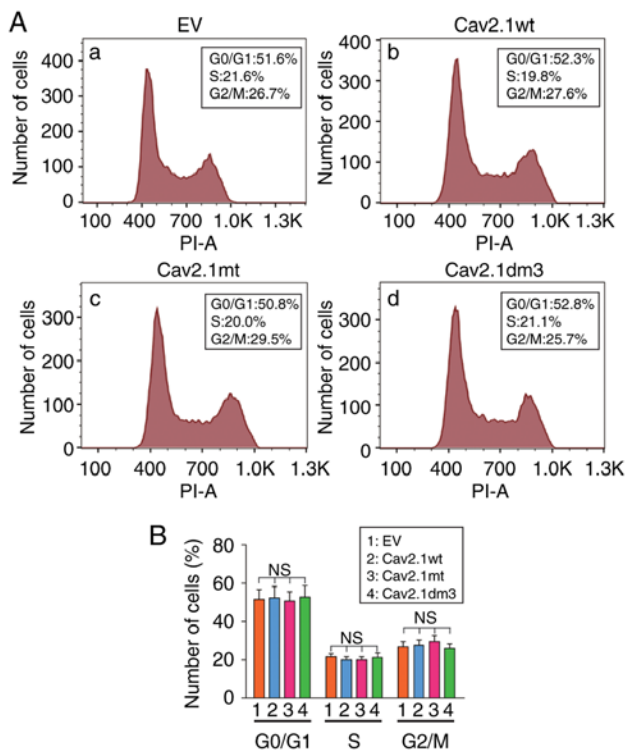


Figure 3. The forced expression of Cav2.1 mt molecules do not affect the cell cycle distribution of the SH-SY5Y cells. (A) The cell cycle was analyzed by flow cytometry and the results indicated that compared with the EV and Cav2.1 wt groups, Cav2.1 mt and Cav2.1dm3 transfectants exhibited no difference in cell cycle distribution. (B) Statistical result of the cell cycle distribution. No difference in cell cycle distribution was observed among EV, Cav.1 wt, Cav2.1 mt and Cav2.1dm3 (Tukey's test). Cav2.1 mt, mutant-type Cav2.1; Cav.1 wt, wild-type Cav2.1; EV, empty vector; NS, no significance.

the cell proliferation of the SH-SY5Y cells. Conversely, the forced expression of Cav2.1dm1, Cav2.1dm2 and Cav2.1dm3, containing 26 polyQ repeats, significantly impaired cell proliferation (Fig. 2C, $P < 0.01$). Notably, the Cav2.1dm3 transfectants had the lowest proliferation (Fig. 2C).

Since the Cav2.1dm3 molecule is composed by Q26 and Cav2.1C, and Cav2.1C itself does not affect cell proliferation, therefore it was speculated that Q26 plays a critical role in the Cav2.1-induced cell growth inhibition. To ascertain our hypothesis, another two plasmids were further constructed. Cav2.1dm4, aa2127 to aa2344 of Cav2.1 mt, contains 26 polyQ repeats and ends at the last Q, with no Cav2.1 C-terminus. Cav2.1dm5 is the reversed arrangement of Q26 (aa2319-2344) and Cav2.1C (aa2345-2525). After transfection, it was revealed that neither Cav2.1dm4 nor Cav2.1dm5 affected the cell growth of the SH-SY5Y cells (Fig. 2D, $P > 0.05$). These data indicated that: i) The expanded mutation of the polymorphic Q repeat tract, e.g., from 13 repeats to 26 repeats, has cytotoxicity and impairs the cell growth of the SH-SY5Y cells; and ii) the Q26 tract must be linked with the Cav2.1 C-terminus in a *cis*-arrangement to exert its biological function.

It was surmised that the structure of the glutamine-expanded Cav2.1 is unstable, and the mutant protein cleaves and generates truncated molecules. Therefore the 3D structure of the truncated Cav2.1 beginning with Q13 and Q26 (Fig. 2E) was compared using an online tool (<http://zhanglab.ccmb.med.umich.edu/>). Because the website has set a limit on the amino

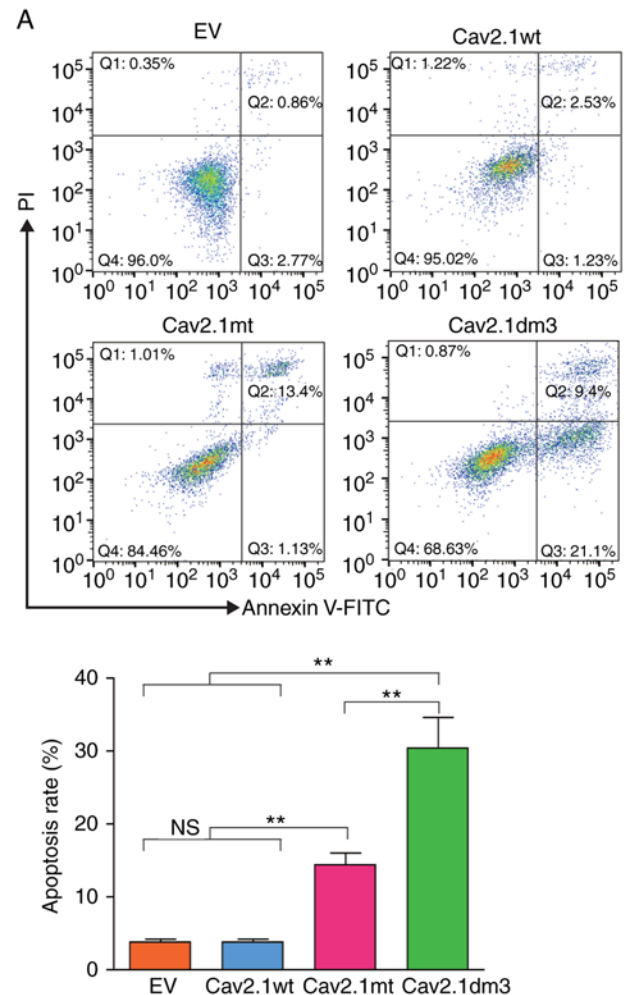


Figure 4. The forced expression of Cav2.1 mt and Cav2.1dm3 induces cell apoptosis in SH-SY5Y cells. (A) The flow cytometric result indicated that compared with the Cav2.1 wt and EV groups, the forced expression of Cav2.1 mt and Cav2.1dm3 significantly induced cell apoptosis in SH-SY5Y cells. $**P < 0.01$, a significant difference in cell apoptosis was observed between EV/Cav2.1 wt and Cav2.1 mt/Cav2.1dm3, and Cav2.1 mt and Cav2.1dm3. NS, no difference in cell apoptosis was observed between EV and Cav2.1 wt (Tukey's test). (B) Cell morphology also revealed that Cav2.1 mt and Cav2.1dm3 markedly induced cell apoptosis. Cav2.1 mt, mutant-type Cav2.1; Cav.1 wt, wild-type Cav2.1; EV, empty vector; NS, no significance.

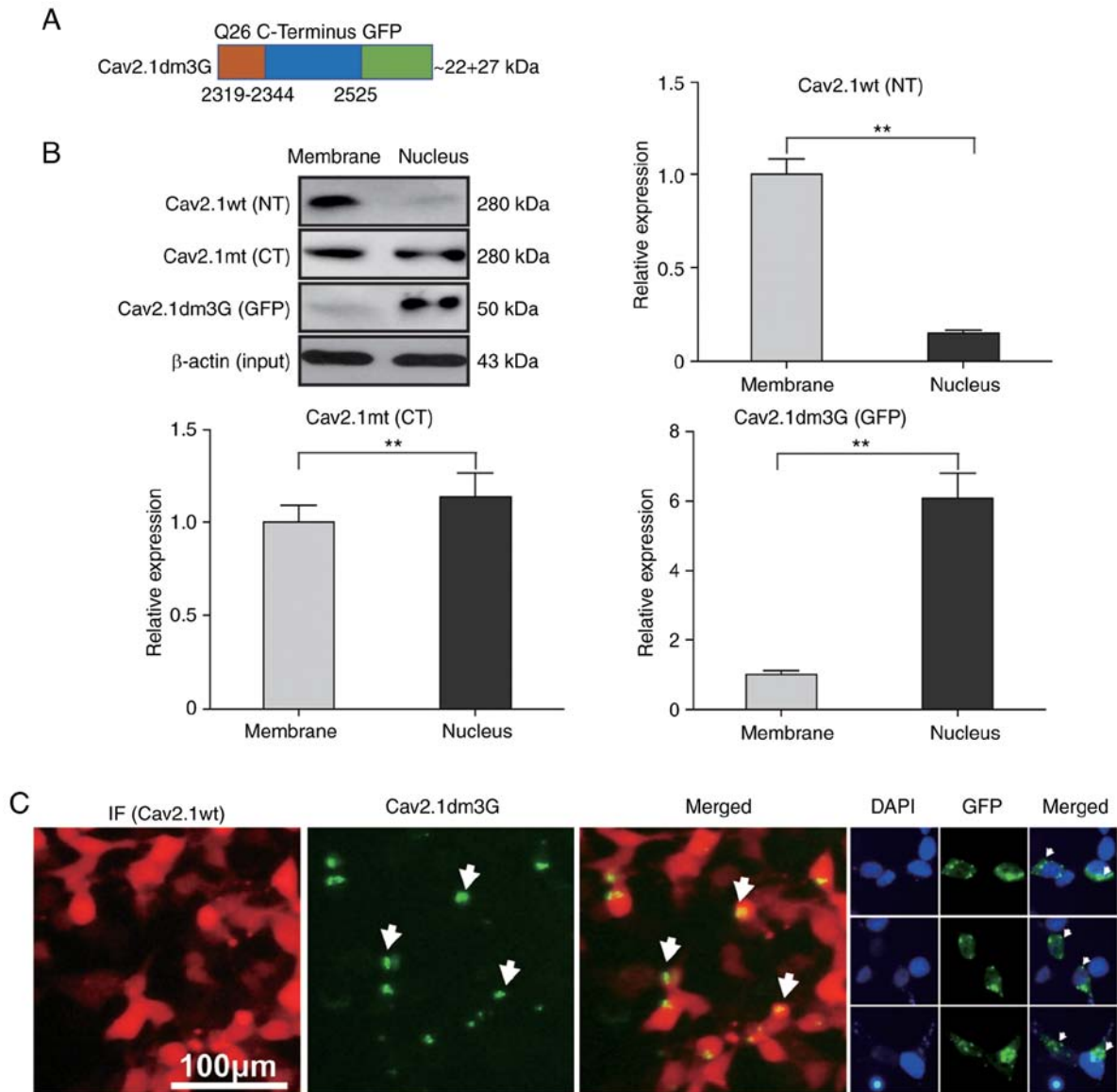


Figure 5. Cav2.1 mutant molecules are translocated to the nucleus of the SH-SY5Y cells. Plasmids expressing Cav2.1 wt, Cav2.1 mt and Cav2.1dm3G were transfected into SH-SY5Y cells, and proteins were collected from cell membranes or the nucleus and were detected by western blotting. (A) Diagram of the Cav2.1dm3-GFP fusion molecule. (B) Western blotting indicated that Cav2.1 wt molecules were located on the cell membrane, Cav2.1 mt molecules were located on both the cell membrane and in the cell nucleus, and Cav2.1dm3G molecules were translocated to the cell nucleus. β -actin was used to illustrate that the membrane proteins and nucleoproteins were extracted from the same quantity of transfected cells. Upper left panel, bands on the blotting membrane; the other panels, relative band density (t-test). (C) Immunofluorescence staining revealed the nuclear translocation phenomenon of Cav2.1 mt molecules. Cav2.1 mt, mutant-type Cav2.1; Cav.1 wt, wild-type Cav2.1; NT, N terminus; CT, C terminus. ** $P < 0.01$.

acid quantity, the 3D structures of the two molecules with 195aa and 208aa are only presented. As revealed in Fig. 2F, the structures of the molecules with Q13 and Q26 at the N-terminus of the truncated Cav2.1 were quite different.

Truncated Cav2.1 does not affect the cell cycle distribution of the SH-SY5Y cells. To elucidate the anti-proliferation mechanisms of the truncated Cav2.1, a cell cycle assay was performed using flow cytometry. However, no variation of cell cycle distribution was observed among the EV, Cav2.1 wt, Cav2.1 mt and Cav2.1dm3 transfectants (Fig. 3, $P > 0.05$).

Truncated Cav2.1 promotes apoptosis of the SH-SY5Y cells. Subsequently, a cell apoptosis assay was performed using flow cytometry. As revealed in Fig. 4, compared to the Cav2.1 wt

and EV transfection groups, the forced expression of Cav2.1 mt and Cav2.1dm3 in SH-SY5Y cells significantly induced apoptosis. The apoptotic rate of the Cav2.1dm3 group was 30.5%, significantly higher than that of 14.53% in the Cav2.1 mt group (Fig. 4A, $P < 0.01$). The cell morphology also indicated the increased apoptosis in the Cav2.1dm3 transfectants (Fig. 4B).

Truncated Cav2.1 molecules are translocated to the nucleus of the SH-SY5Y cells. To gain deeper insight into the role of the truncated Cav2.1 mt molecules in cell apoptosis, a Cav2.1dm3 and GFP fusion molecule was constructed. To avoid impairing the Q26 bioactivity, GFP was fused to the C-terminus of Cav2.1dm3, and named Cav2.1dm3G (Fig. 5A). After the plasmid was delivered into SH-SY5Y cells, the expression of Cav2.1dm3G was detected by western blotting.

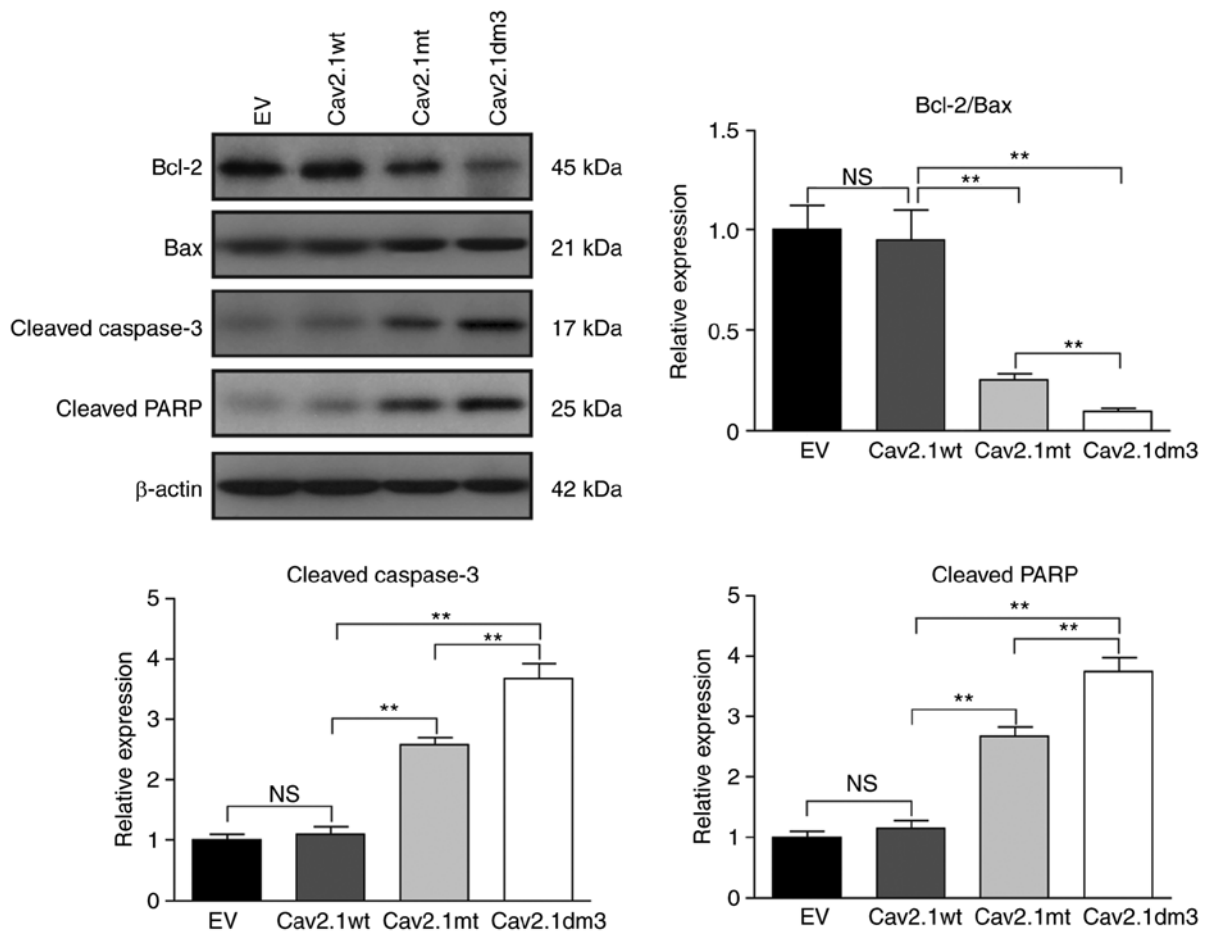


Figure 6. Cav2.1 mt molecules induce cell apoptosis via the Bcl-2/Bax, caspase-3 and PARP pathways. SH-SY5Y cells were transfected with empty vector, Cav2.1 wt, Cav2.1 mt and Cav2.1dm3 plasmid and the levels of Bcl-2, Bax, cleaved caspase-3 and cleaved PARP were detected by western blotting. Upper left panel, western blot result indicated that Cav2.1 mt molecules activated the Bcl-2/Bax, caspase-3 and PARP apoptotic pathways. The other panels, relative band density (Tukey's test). **P<0.01. Cav2.1 mt, mutant-type Cav2.1; Cav1 wt, wild-type Cav2.1; PARP, poly ADP-ribose polymerase; EV, empty vector; NS, no significance.

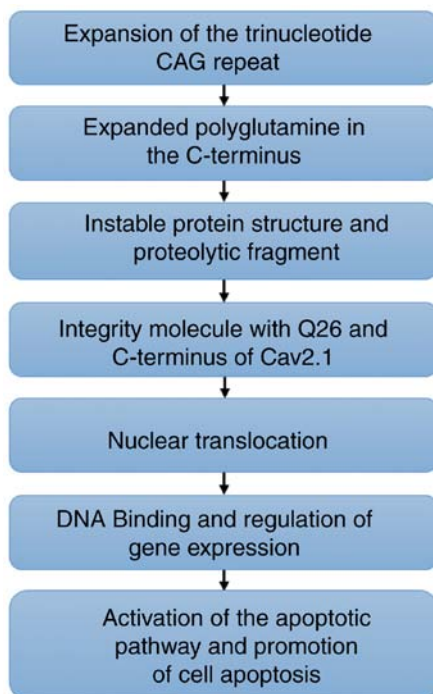


Figure 7. The putative mechanism of the Cav2.1 mutation-induced cell apoptosis in nerve cells.

As controls, the expression of Cav2.1 wt and Cav2.1 mt in the transfectants were also detected by western blotting, concurrently. As revealed in Fig. 5B, the western blot results revealed that the Cav2.1 wt molecules were mainly located on the cell membrane (87.0%, the upper right panel, P<0.01), Cav2.1 mt molecules were located both on the cell membrane and in the cell nucleus (46.7% vs. 53.3%, the left lower panel, P<0.05), whereas most Cav2.1dm3G molecules were located in the cell nucleus (85.9%, the right lower panel, P<0.01).

A cell immunofluorescence staining experiment was also performed and it was observed that the Cav2.1 wt molecules were distributed on the cell membrane, whereas the GFP fluorescence of Cav2.1dm3G molecules was mainly distributed inside the cell nucleus (Fig. 5C). These data indicated that the truncated Cav2.1 mt molecules were translocated to nucleus, increasing apoptosis of the SH-SY5Y cells.

Truncated Cav2.1 mt induces cell apoptosis via the Bcl-2/Bax/caspase-3/PARP pathway. It has been reported that polyQ interacts with the mitochondrial apoptotic pathway and caspase apoptotic proteins to exert cytotoxicity (15). Therefore, the expression of Bcl-2, Bax, cleaved caspase-3 and cleaved PARP were detected. Western blot results revealed that the Bcl-2/Bax ratio was markedly decreased in Cav2.1 mt

and Cav2.1dm3 transfectants (Fig. 6, upper left and upper right panel, $P < 0.01$). The caspase-3 and PARP cell apoptotic pathways were also activated (Fig. 6 upper left panel, lower left/right panel, $P < 0.01$).

Discussion

PME comprises a group of rare neurodegenerative disorders characterized by ataxia, myoclonus, seizures, and progressive cognitive impairment (16). The occurrence and development of PME is always accompanied by certain types of gene mutations. Tonin *et al* identified a newly discovered synonymous c.363A>G (Gly82Gly) mutation in the β -glucosidase (*GBA*) gene in a type 3 Gaucher disease patient that causes the loss of an exon splicing enhancer (17). He *et al* revealed a novel c.995-1G>A homozygous splicing mutation in the *SCARB2* gene in two PME patients that leads to loss of function of the *SCARB2* protein (18).

In recent years, an increasing number of mutations in the *CACNA1A* gene have been reported as causative factors for several types of neurological disorders. Using next-generation sequencing, Grieco *et al* identified an R2157G missense variant in a Moroccan hemiplegic migraine patient and an I1512T missense variation in patients with FHM (6). Using whole-exome sequencing, Khaiboullina *et al* identified an R583Q missense mutation in patients with FHM (5). Algahtani *et al* summarized that there are more than 170 disease-causing variants of *CACNA1A*, including mutations with small deletions, gross deletions, missense variants, nonsense variants, splice variants, small insertions, complex rearrangements and repeat variations (19).

In a previous study, using whole-exome sequencing, we identified a homozygous variant in PME patients: a repeated CAG mutation in the *CACNA1A* gene, which encodes an elongated tract of glutamine residues in the C-terminus of the Cav2.1 protein. Although the intranuclear accumulation of mutant proteins with an expanded polyQ tract has been well established, the relationship between neurotoxicity and glutamine aggregation remains to be investigated. In the present study, it was revealed that the Cav2.1 protein with Q26 was translocated to the nucleus of the SH-SY5Y cells. By constructing a series of truncated molecules, it was revealed that overexpression of the Cav2.1 protein with a Q26 mutation in the C-terminus induced cell apoptosis. Notably, the shorter the truncated molecule was, the more obvious the cell toxicity was found to be. Gerhardstein *et al* reported that Cav1.2, an L-type voltage-gated calcium channel, was proteolytically cleaved in neurons and cardiac myocytes, yielding a truncated channel and a cytoplasmic C-terminal fragment (20). Gomez-Ospina *et al* reported that a high level of the C-terminal Cav1.2 fragment was localized in the nucleus of brain cells, whereas the N-terminal portion of the channel was localized in the membrane and cytoplasmic fractions (21). Park *et al* reported a frameshift mutation (c.1642del, p.H548Tfs*24) in the *CACNA1A* gene leading to a prematurely truncated Cav2.1 protein (22). Therefore, it was concluded that: i) Cav2.1 and similar voltage-gated proteins tend to be cleaved in the C-terminus due to the unstable protein structure caused by the polyQ fragment; ii) the cleavage yields two (perhaps more) truncated molecules, and the C-terminal fragment tends to translocate to the nucleus; and iii) the

prematurely truncated molecules are generated from either proteolysis or gene mutation.

The truncated voltage-gated proteins may exert their biological function in two ways. Through one mechanism, the truncated fragment binds to gene regulatory elements, e.g., promoters. For instance, Gomez-Ospina *et al* revealed that the C-terminal fragment of Cav1.2 in the nucleus interacted with multiple transcriptional regulators and affected the transcription of a wide variety of endogenous genes important for neuronal signaling and excitability (21). The other mechanism depends on the polyQ structure, which is manifested in a so-called polyQ disease. For example, Huntington's disease is caused by polyQ (more than 35 repeats) in the Huntington protein that results in neuronal cell death (23). In addition, aberrant expression of superoxide dismutase and accumulation of oxidative products were also observed in a CAG-repeat disease (24).

Cell apoptosis is mediated by caspases, which are activated by signals from the plasma membrane and mitochondria. Bcl-2/Bax is the key mitochondrial apoptotic pathway controlling cell apoptosis. Sanchez *et al* reported that the polyglutamine repeat (Q79)/caspase 8 axis-induced cell death was critical in Huntington's disease (25). Tien *et al* demonstrated that the polyglutamine repeat (Q26 and Q78) may decrease the mRNA level of Bcl-2 in Machado-Joseph disease cells (26). In the present study, it was revealed that the truncated Cav2.1 mutant molecule induced cell apoptosis through the activation of the Bcl-2/Bax, caspase-3 and PARP pathways. The production of PAR chains by PARPs is one of the first steps in the process of DNA damage repair (27). In addition, the increased level of cleaved caspase-3 can lead to cleaved PARP, which is an inactive form, thereby disrupting DNA repair and resulting in apoptosis (28). Considering the relationship among Bcl-2/Bax, caspase-3 and PARP, the present results are reasonable. However, since few investigations have focused on the correlation between polyQ and PARP, to support our conclusion, further experiments are required.

In summary, in the present study, it was demonstrated that an aberrant elongated tract of polyQ in the Cav2.1 protein may proteolytically generate a short fragment that is translocated to the nucleus, inducing cell apoptosis in human SH-SY5Y cells (Fig. 7). The present study may provide new insights for the interpretation of the pathogenesis of PME and for the relationship among polyQ, *CACNA1A* gene mutation and PME.

Acknowledgements

We would like to thank Professor Dehai Yu at The Laboratory of Cancer Precision Medicine of the First Hospital of Jilin University for revising this article critically for important intellectual content.

Funding

The present study was supported in part by grants from the Translational-and-Clinical Collaborative Research Project from the First Hospital of Jilin University (grant no. 2018-ZL-12 to YL); the National Natural Science Foundation of China (grant no. 81701270 to YL); the Transformation Fund of the First Hospital of Jilin University (grant no. JDYYZH-1902033

to YL); the Health Special Fund from Jilin Province Department of Finance (grant no. 2018SCZWSZX-048 to XS).

Availability of data and materials

The datasets used and analyzed during the current study are available from the corresponding author on reasonable request.

Authors' contributions

DM and YL contributed to the conception and design of the study. JS and XS contributed to the acquisition, analysis and interpretation of data. JS drafted the manuscript. XS and ZL analyzed the data and was involved in performing the experiments. All authors have read and approved the final manuscript.

Ethics approval and consent to participate

Not applicable.

Patient consent for publication

Not applicable.

Competing interests

The authors declare that they have no competing interests.

References

- Ophoff RA, Terwindt GM, Vergouwe MN, van Eijk R, Oefner PJ, Hoffman SM, Lamerdin JE, Mohnweiser HW, Bulman DE, Ferrari M, *et al*: Familial hemiplegic migraine and episodic ataxia type-2 are caused by mutations in the Ca²⁺ channel gene CACNL1A4. *Cell* 87: 543-552, 1996.
- Lea RA, Curtain RP, Hutchins C, Brimage PJ and Griffiths LR: Investigation of the CACNA1A gene as a candidate for typical migraine susceptibility. *Am J Med Genet* 105: 707-712, 2001.
- Petrovicova A, Brozman M, Kurca E, Gobo T, Dluha J, Kalmarova K, Nosal V, Hikkelova M, Krajciová A, Burjanivova T and Sivak S: Novel missense variant of CACNA1A gene in a Slovak family with episodic ataxia type 2. *Biomed Pap Med Fac Univ Palacky Olomouc Czech Repub* 161: 107-110, 2017.
- Bavassano C, Eigentler A, Stanika R, Obermair GJ, Boesch S, Dechant G and Nat R: Bicistronic CACNA1A gene expression in neurons derived from spinocerebellar ataxia type 6 patient-induced pluripotent stem cells. *Stem Cells Dev* 26: 1612-1625, 2017.
- Khaiboullina SF, Mendelevich EG, Shigapova LH, Shagimardanova E, Gazizova G, Nikitin A, Martynova E, Davidyuk YN, Bogdanov EI, Gusev O, *et al*: Cerebellar atrophy and changes in cytokines associated with the CACNA1A R583Q mutation in a Russian familial hemiplegic migraine type 1 family. *Front Cell Neurosci* 11: 263, 2017.
- Grieco GS, Gagliardi S, Ricca I, Pansarasa O, Neri M, Gualandi F, Nappi G, Ferlini A and Cereda C: New CACNA1A deletions are associated to migraine phenotypes. *J Headache Pain* 19: 75, 2018.
- Lv Y, Wang Z, Liu C and Cui L: Identification of a novel CACNA1A mutation in a Chinese family with autosomal recessive progressive myoclonic epilepsy. *Neuropsychiatr Dis Treat* 13: 2631-2636, 2017.
- Zhang Q, Chen ZS, An Y, Liu H, Hou Y, Li W, Lau KF, Koon AC, Ngo JCK and Chan HYE: A peptidyl inhibitor for neutralizing expanded CAG RNA-induced nucleolar stress in polyglutamine diseases. *RNA* 24: 486-498, 2018.
- Roshan R, Choudhary A, Bhambri A, Bakshi B, Ghosh T and Pillai B: MicroRNA dysregulation in polyglutamine toxicity of TATA-box binding protein is mediated through STAT1 in mouse neuronal cells. *J Neuroinflammation* 14: 155, 2017.
- von Niederhausern N, Ducray A, Zielinski J, Murbach M and Mevisen M: Effects of radiofrequency electromagnetic field exposure on neuronal differentiation and mitochondrial function in SH-SY5Y cells. *Toxicol In Vitro* 61: 104609, 2019.
- Karikari TK, Nagel DA, Grainger A, Clarke-Bland C, Crowe J, Hill EJ and Moffat KG: Distinct conformations, aggregation and cellular internalization of different tau strains. *Front Cell Neurosci* 13: 296, 2019.
- Liu M, Bai X, Yu S, Zhao W, Qiao J, Liu Y, Zhao D, Wang J and Wang S: Ginsenoside Re inhibits ROS/ASK-1 dependent mitochondrial apoptosis pathway and activation of Nrf2-Antioxidant response in beta-amyloid-challenged SH-SY5Y cells. *Molecules* 24: E2687, 2019.
- Livak KJ and Schmittgen TD: Analysis of relative gene expression data using real-time quantitative PCR and the 2(-Delta Delta C(T)) method. *Methods* 25: 402-408, 2001.
- Kordasiewicz HB, Thompson RM, Clark HB and Gomez CM: C-termini of P/Q-type Ca²⁺ channel alpha1A subunits translocate to nuclei and promote polyglutamine-mediated toxicity. *Hum Mol Genet* 15: 1587-1599, 2006.
- Tsoi H, Lau TC, Tsang SY, Lau KF and Chan HY: CAG expansion induces nucleolar stress in polyglutamine diseases. *Proc Natl Acad Sci USA* 109: 13428-13433, 2012.
- Mizuguchi T, Suzuki T, Abe C, Umemura A, Tokunaga K, Kawai Y, Nakamura M, Nagasaki M, Kinoshita K, Okamura Y, *et al*: A 12-kb structural variation in progressive myoclonic epilepsy was newly identified by long-read whole-genome sequencing. *J Hum Genet* 64: 359-368, 2019.
- Tonin R, Catarzi S, Caciotti A, Procopio E, Marini C, Guerrini R and Morrone A: Progressive myoclonus epilepsy in gaucher disease due to a new Gly-Gly mutation causing loss of an exonic splicing enhancer. *J Neurol* 266: 92-101, 2019.
- He J, Lin H, Li JJ, Su HZ, Wang DN, Lin Y, Wang N and Chen WJ: Identification of a novel homozygous splice-site mutation in SCARB2 that causes progressive myoclonus epilepsy with or without renal failure. *Chin Med J (Engl)* 131: 1575-1583, 2018.
- Algahtani H, Shirah B, Algahtani R, Al-Qahtani MH, Abdulkareem AA and Naseer MI: A novel mutation in CACNA1A gene in a Saudi female with episodic ataxia type 2 with no response to acetazolamide or 4-aminopyridine. *Intractable Rare Dis Res* 8: 67-71, 2019.
- Gerhardstein BL, Gao T, Bunemann M, Puri TS, Adair A, Ma H and Hosey MM: Proteolytic processing of the C terminus of the alpha(1C) subunit of L-type calcium channels and the role of a proline-rich domain in membrane tethering of proteolytic fragments. *J Biol Chem* 275: 8556-8563, 2000.
- Gomez-Ospina N, Tsuruta F, Barreto-Chang O, Hu L and Dolmetsch R: The C terminus of the L-type voltage-gated calcium channel Ca(V)_{1.2} encodes a transcription factor. *Cell* 127: 591-606, 2006.
- Park D, Kim SH, Lee YJ, Song GJ and Park JS: A novel CACNA1A mutation associated with episodic ataxia 2 presenting with periodic paralysis. *Acta Neurol Belg* 118: 137-139, 2018.
- Walker FO: Huntington's disease. *Lancet* 369: 218-228, 2007.
- Miyata R, Hayashi M, Tanuma N, Shioda K, Fukatsu R and Mizutani S: Oxidative stress in neurodegeneration in dentatorubral-pallidoluysian atrophy. *J Neurol Sci* 264: 133-139, 2008.
- Sanchez I, Xu CJ, Juo P, Kakizaka A, Blenis J and Yuan J: Caspase-8 is required for cell death induced by expanded polyglutamine repeats. *Neuron* 22: 623-633, 1999.
- Tien CL, Wen FC and Hsieh M: The polyglutamine-expanded protein ataxin-3 decreases bcl-2 mRNA stability. *Biochem Biophys Res Commun* 365: 232-238, 2008.
- Maiuri T, Stuart CE, Hung CLK, Graham KJ, Barba Bazan CA and Truant R: DNA damage repair in huntington's disease and other neurodegenerative diseases. *Neurotherapeutics* 16: 948-956, 2019.
- Hwang JY, Park JH, Kim MJ, Kim WJ, Ha KT, Choi BT, Lee SY and Shin HK: Isolinderalactone regulates the BCL-2/caspase-3/PARP pathway and suppresses tumor growth in a human glioblastoma multiforme xenograft mouse model. *Cancer Lett* 443: 25-33, 2019.



This work is licensed under a Creative Commons Attribution-NonCommercial-NoDerivatives 4.0 International (CC BY-NC-ND 4.0) License.